

# We are IntechOpen, the world's leading publisher of Open Access books Built by scientists, for scientists

6,900

Open access books available

185,000

International authors and editors

200M

Downloads

Our authors are among the

154

Countries delivered to

TOP 1%

most cited scientists

12.2%

Contributors from top 500 universities



WEB OF SCIENCE™

Selection of our books indexed in the Book Citation Index  
in Web of Science™ Core Collection (BKCI)

Interested in publishing with us?  
Contact [book.department@intechopen.com](mailto:book.department@intechopen.com)

Numbers displayed above are based on latest data collected.  
For more information visit [www.intechopen.com](http://www.intechopen.com)



# Brain Computer Interface Based on the Flash Onset and Offset Visual Evoked Potentials

Po-Lei Lee<sup>1,2</sup>, Yu-Te Wu<sup>2</sup>, Kuo-Kai Shyu<sup>1</sup> and Jen-Chuen Hsieh<sup>2</sup>

<sup>1</sup>*Department of Electrical Engineering, National Central University,*

<sup>2</sup>*Institute of Brain Science, National Yang-Ming University,  
Taiwan*

## 1. Introduction

Severe motor disabilities can limit one's ability in communication, especially for patients suffering from amyotrophic lateral sclerosis (ALS), severe cerebral palsy, head trauma, multiple sclerosis, and muscular dystrophies who are incapable of conveying their intentions (locked-in syndrome) to the external environment. For the last several decades, a considerable amount of research effort has been devoted towards the development of novel communication techniques which are independent of peripheral nerves and muscles. One promising method is the use of neural activities, for example, electroencephalography (EEG) or intracortical neural activities, arising from the human brain, as control or communication signals. Such techniques are referred to as 'brain computer interfaces' (BCIs) (Wolpaw et al., 2000).

Several EEG-based BCI systems have been developed with elaborately designed paradigms to induce endogenous or exogenous neuroelectric signals which were detected and translated into control signals for communication purposes. Endogenous BCI communicates with environments independent of sensory responses or muscles which enable users to control external environments directly. For examples, Pfurtscheller et al. (2000) measured sensorimotor mu rhythms during subject's imagery movements and achieved a high recognition rate of 90%; Blankertz et al. (2007) constructed Berlin Brain-Computer Interface (BBCI) with high ITR (>35 bits/min) based on detections of the modulations of sensorimotor rhythms due to motor imagery; Birbaumer et al. (1999) developed a Thought Translation Device (TTD) to measure slow cortical potentials (SCPs) for a binary selection task; Mason & Birch (2000) designed an asynchronous detector to control a binary switch by using the detected motor-related potentials (MRPs) filtered within 1-4 Hz. However, the ITRs of endogenous BCIs are relatively low (between 5 and 25 bits/min) because the performance of translation algorithm in extracting reliable features can be easily degraded by the undesired characteristics of neuroelectric signals, such as artifacts, task-unrelated EEG, and large variability in latencies. Besides, the subjects participated in the endogenous BCIs usually require extensive training for generating specific patterns. The exogenous BCIs, on the contrary, require parts of user's sensation ability involved in a stimulating environment to induce sensory neurophysiological activities, such as P300-based (Donchin et al., 2000; Meinicke et al., 2003), VEP (visual evoked potential)-based (Lee et al., 2005; Lee et al., 2006; Sutter, 1992), SSVEP (steady-state visual evoked potential)-based (Cheng et al., 2002; Cheng

et al., 2006; Kelly et al., 2005; Middendorf et al., 2000; Trejo et al., 2006) and SSSEP (steady-state somatosensory evoked potential)-based systems (Muller-Putz et al., 2006). Neurophysiological activities induced from sensation inputs are self-regulated by the users with specific patterns which can be easily distinguished to achieve high ITRs (>25 bits/min). Especially, the ITRs of P300-based and VEP-based BCIs can be as high as 50.5 bits/min (Meinicke et al., 2003) and 43 bits/min (Wang et al., 2006), respectively, with the aid of support vector machine and bipolar channel design.

BCI systems with high information transfer rates (ITRs) require fast-responding bio-signals and a reliable translation algorithm to convert such signals into control commands. Visual stimulation using flashes of light is a popular and easy means to elicit flash visual evoked potentials (FVEPs) with short latencies short enough to be useful in a BCI. Specifically, FVEP manifests four major peaks: N1, P1, N2, and P2, with latencies less than 200 ms after flash onset or offset (Spehlmann, 1985). In the present study, an exogenous BCI system was developed for users who have sensitive visual acuity (e.g., users are capable of distinguishing two objects in space with 3° visual angle apart). The proposed BCI was constructed based on the central flash FVEPs, which were induced from abrupt light onsets and offsets, to generate control signals with high ITR. When the subjects pay their attention on the target and according to the neural connections and interactions of the route from the retina to the primary visual cortex, visual stimuli at central visual fields can generate the so-called 'cortical magnification' which makes the central FVEPs more prominent than any FVEPs evoked from peripheral visual fields (Odom et al., 2004; Sutter, 1992). In order to remove the contamination of peripheral FVEPs from central FVEPs, we designed flickering sequences with mutually independent flash onsets (or offsets) generated by random ON and OFF durations. Since FVEP in human visual cortex is time-locked and phase-locked to the timing of flash onset (or offset) (Spehlmann, 1985), EEG data segmented based on the flash onset (or offset) timing of one chosen flickering sequence will contain time-locked FVEPs of the chosen flickering sequence mixed with non-time-locked FVEPs induced from other flickering sequences. By applying a simple averaging process, the intentionally manipulated time-locked and non-time-locked properties conduce the time-locked FVEPs to being enhanced concurrently with the suppression of non-time-locked FVEPs. After comparing the averaged onset and offset responses and referring to the characteristic of "cortical magnification", the stimulus producing the onset and offset FVEPs with the largest peak-to-valley features was identified as the gazed target. The flickering sequences with mutually independent flash onsets (or offsets) will be termed as "mutually independent flickering sequences" in the followings for convenience purpose.

Some other VEP-based BCI systems have been proposed in recent years. Two of them were gaze-dependent systems, one was based on the fast multifocal visual evoked potential (FMFVEP) (Sutter, 1992) and the other on the steady-state visual evoked potential (SSVEP) (Cheng et al., 2002). The flickering stimuli of FMFVEP-based system were generated by a pseudo-random binary sequence with a fixed time lag between any two adjacent channels. Each entire pseudo-random sequence was convoluted with a standard VEP response to create a so-called "expected response". By finding the maximum correlation between the measured EEG signals and the expected response of each flickering stimulus, the gazed stimulus was recognized. Instead of using a binary sequence with fixed flickering frequency, each stimulus in the SSVEP-based system was designed to have its own flickering frequency. The gazed target was identified by finding the stimulus which contributes maximum power of SSVEP at Fourier spectrum. However, there are limitations in these two

gaze-dependent systems. The FMFVEP-based method presumed identical response of VEP across all trials and used it as template in correlation computation (Sutter, 1992). Such a stringent assumption was irreconcilable with the truth (Jung et al., 2001; Tang et al., 2002) and the resultant correlation may not be optimal in detecting the gazed target. In the SSVEP-based method, the flickering frequencies were confined to be lower than 14 Hz due to the frame rate of PC monitor, and flickering frequencies around alpha band should also be excluded to avoid the interference of spontaneous alpha rhythm (Salmelin and Hari, 1994). These two constraints may reduce the available flickering channels and communication bandwidth.

Another type of VEP-based BCI system requests users to pay attention to flickering stimuli for regulating the SSVEP responses (Kelly et al., 2005; Trejo et al., 2006). The operation of such attention-regulated SSVEP systems is independent of eye movements, which is suitable for users who have well-preserved visual acuity but are incapable of moving their eyes. Nevertheless, the attention-regulated SSVEP systems are usually designed with few flickering channels (FCs) since too many FCs may distract user's attention and result in poor performance. Besides, attention maintenance in operating the system relies on user's experience and it usually requires users to take a training procedure (e.g., 3 minutes) before they can achieve accuracies higher than 80% (Trejo et al., 2006). Another problem is the evaluation of system performance. Owing to the inter-individual variations on attention maintenance and time lag for successful attention modulation, Trejo et al. (2006) reported that the lag for each attention modulated SSVEP was in a range of 1~5 seconds which limited the bandwidth of ITR.

The current system, originated from our previous BCI work in which only the flash-onset induced VEP was employed (Lee et al., 2005; Lee et al., 2006), was designed by taking the additional distinguishable feature from offset FVEP into account, not only to improve the detection accuracy of gazed stimuli but also achieve better ITR.

## 2. Materials and methods

### 2.1 Visual stimuli and task

The visual stimuli were presented on a 17-inch ViewSonic LCD monitor (model VG724; reaction time < 3 ms; 60 frames/s) with a distance of 40~50 centimeters away from the viewer. The full screen was partitioned into several flickering channels. Each flickering channel (FC) was designed to be a rectangle (subtended angle = 3°) overlaid with a small cross-hair and driven by a flickering sequence consisting of alternative ON and OFF (illumination-extinction) states. The small cross hairs were used to draw subjects' attention so that subjects could fixate their gaze at the centers of the FCs. The luminance of ON and OFF state in each FC were 168.7 candelas (cd/m<sup>2</sup>) and 8.1 cd/m<sup>2</sup>, respectively, measured by a luminance meter (LS-110; Konica Minolta Photo Imaging Inc., USA) resulting in Michelson contrast of 90.3 %. Duration of each ON or OFF state was a concatenation of two segments, one with a fixed length of 116.7 ms (7 frames) and the other with a variable length which was uniformly distributed between 0 ms and 233.3 ms (0~14 frames). In other words, the duration of each ON or OFF state was between 116.7 and 350 ms and its mean is 233.3 ms. Of note is that the fixed duration was designed to prevent the major visual response of current onset or offset FVEP overlapped with the incoming offset or onset FVEP, and the random duration was used to generate temporal independence of flash onsets (or offsets) among different flickering sequences (see Discussion section).

To demonstrate the stability and applicability of the proposed FVEP system, one control study and one application study were designed and tested. In the control study, 25 FCs, namely from FC-1 to FC-25, were presented in an arrangement of  $5 \times 5$  grid (see Fig. 1A). Subjects were asked to gaze binocularly at the center of each FC for one-minute recording. In the application study, 12 flickering channels were displayed as a pseudo telephone keypad consisting of ten digits '0-9', one Backspace 'B' and one Enter 'E' (see Fig. 1B). The Backspace 'B' was reserved for the future use of correcting error input and was not used in the study. Subjects were asked to stare at the target stimuli one by one until the most prominent central onset and offset FVEPs could be detected for the identification of gazed stimulus. A representative digit or a letter was sent out right after recognition of gazed-stimulus. All subjects were instructed to complete a string: 0287513694E.

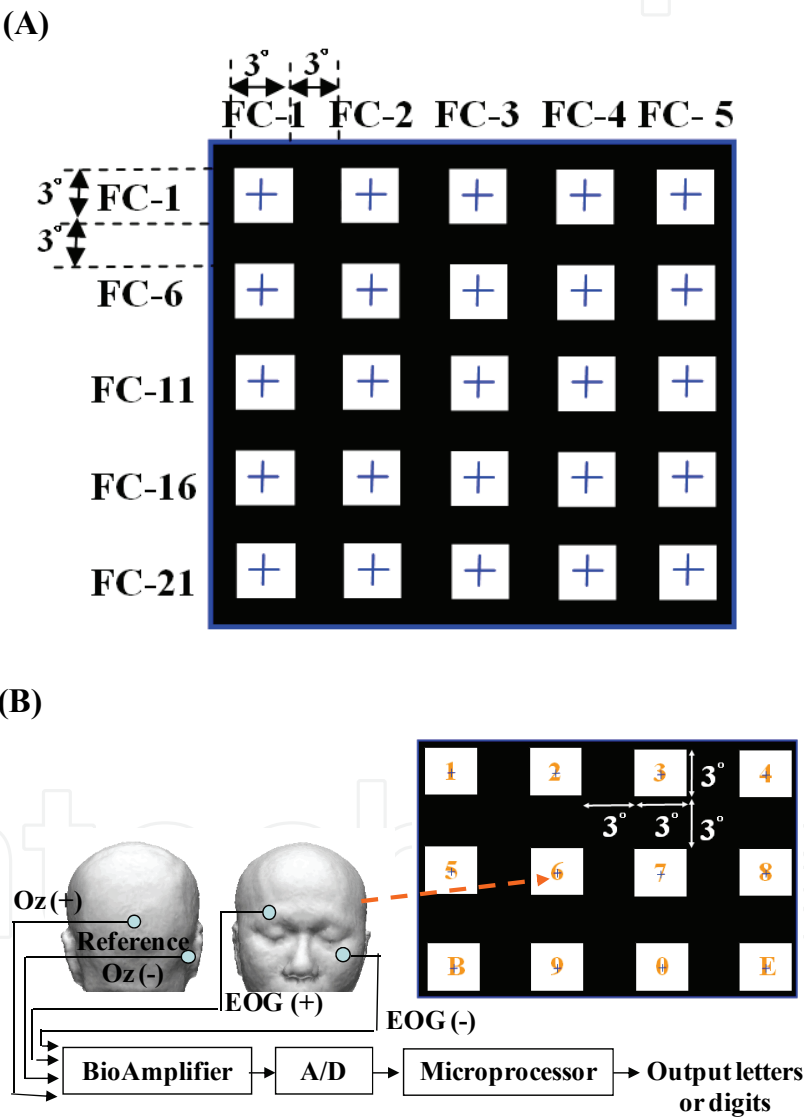


Fig. 1. The visual stimuli used in inducing onset and offset FVEPs. (A) 25 flickering channels, labeled by FC-1, ..., FC-25, were presented in a  $5 \times 5$  grid in the control study. (B) 12 flickering channels were designed as a pseudo telephone keypad consisting of 10 digits '0-9', one Backspace 'B' and one Enter 'E' in the application study. One EEG channel at the Oz position and the other reference electrode at the right mastoid were utilized.



## 2.2 Subjects and EEG recordings

Five healthy volunteers (three males and two females), ages from 25 to 32 years, were recruited to participate in our studies. Each subject had corrected Snellen visual acuity of 6/6 or better, with no history of clinical visual disease. All subjects gave informed consent, and the study was approved by the Ethics Committee of Institutional Review Board, Taipei Veterans General Hospital, Taiwan. Two of the five subjects (Subject I and II both were male) had one-hour experience in this visual stimulation task while the other three were naïve subjects. VEPs were recorded with a whole-head 40-channel EEG system (bandpass, 0.05-50 Hz; digitized at 250 Hz; Nu Amplifier; Neuroscan Inc., USA), while subjects sat on a comfortable armchair in a dimly illuminated room. Two out of the 40 EEG channels were respectively used as bipolar horizontal and vertical electro-oculograms (EOG); one was placed below and above the left eye and the other at the bilateral outer canthi. The signals recorded from two additional electrodes placed on left and right mastoids were averaged and used as the reference to all EEG channels. The inter-electrode impedances were kept below 5 K $\Omega$  during recording. It should be noted that the use of whole-head EEG recording in the control study is only for demonstration purpose. In the application study, only one EEG channel was placed at the Oz position (Fisch & Spehlmann, 1999) and another one reference electrode at the right mastoid (see Fig. 1B), rather than using the whole-head EEG. An additional bipolar electroculargraphy (EOG) channel was placed on the upper site of right eye and the lower site of the left eye to monitor eye movements. The threshold level for rejecting artifact-contaminated epochs was set at 100  $\mu$ V in both control and application studies. The EEG recordings were bandpass filtered, within 0.1-50 Hz, to remove 60 Hz and low-frequency drifts, followed by digitization (NI-PCI 6071E, National Instruments). All the aforementioned computations and signal processing procedures presented in the following sections were implemented by the LabVIEW software (National Instruments, USA) to achieve on-line analysis.

## 2.3 Peak-to-valley amplitudes $Amp_{onset}$ and $Amp_{offset}$ in the onset and offset FVEPs

In our study, the flickering stimuli are driven by flickering sequences with ON and OFF alternative states. The FVEPs, induced by flash onsets and offsets, referring to onset FVEP and offset FVEP, respectively, were measured and used as features for detecting gazed stimuli. Both the onset and offset FVEPs have two major negative and two positive peaks within 200 ms after flash onset and offset (Spehlmann, 1985), which were termed as  $N1_{onset}$ ,  $P1_{onset}$ ,  $N2_{onset}$ , and  $P2_{onset}$  in onset FVEP (see Fig. 2A and 2C) and  $N1_{offset}$ ,  $P1_{offset}$ ,  $N2_{offset}$ , and  $P2_{offset}$  in offset FVEP (see Fig. 2B and 2D), respectively. Topographies in subject I (see Fig. 2E and 2F) and subject III (see Fig. 2G and 2H) also demonstrated that the  $P2_{onset}$  and  $P1_{offset}$  were induced from occipital areas. In normal subjects, the  $N2_{onset}$  and  $P2_{onset}$  peaks were usually the most robust (Spehlmann, 1985; Odom et al., 2004). The amplitude difference between  $N2_{onset}$  and  $P2_{onset}$  peaks, denoted by  $Amp_{onset}$ , and that between  $N1_{offset}$  and  $P1_{offset}$  peaks, denoted by  $Amp_{offset}$ , were calculated and their sum,  $Amp_{onset} + Amp_{offset}$ , was used for detecting gazed stimulus. Examples of the onset and offset FVEPs from two subjects were shown in Fig. 2. The latencies of  $N2_{onset}$ ,  $P2_{onset}$ ,  $N1_{offset}$ , and  $P1_{offset}$  peaks were represented by  $t_{onset\_n2}$ ,  $t_{onset\_p2}$ ,  $t_{offset\_n1}$ , and  $t_{offset\_p1}$ , respectively (see Fig. 2C and 2D). Because the presence of the latencies of  $N2_{onset}$ ,  $P2_{onset}$ ,  $N1_{offset}$ , and  $P1_{offset}$  peaks could vary from trial to trial during experiments, the four peaks were searched in a time window by extending  $\pm 15$  ms (Lee et al., 2006) around the timing of the peaks (illustrated by shaded windows in Fig. 2C and 2D) obtained from the control study.

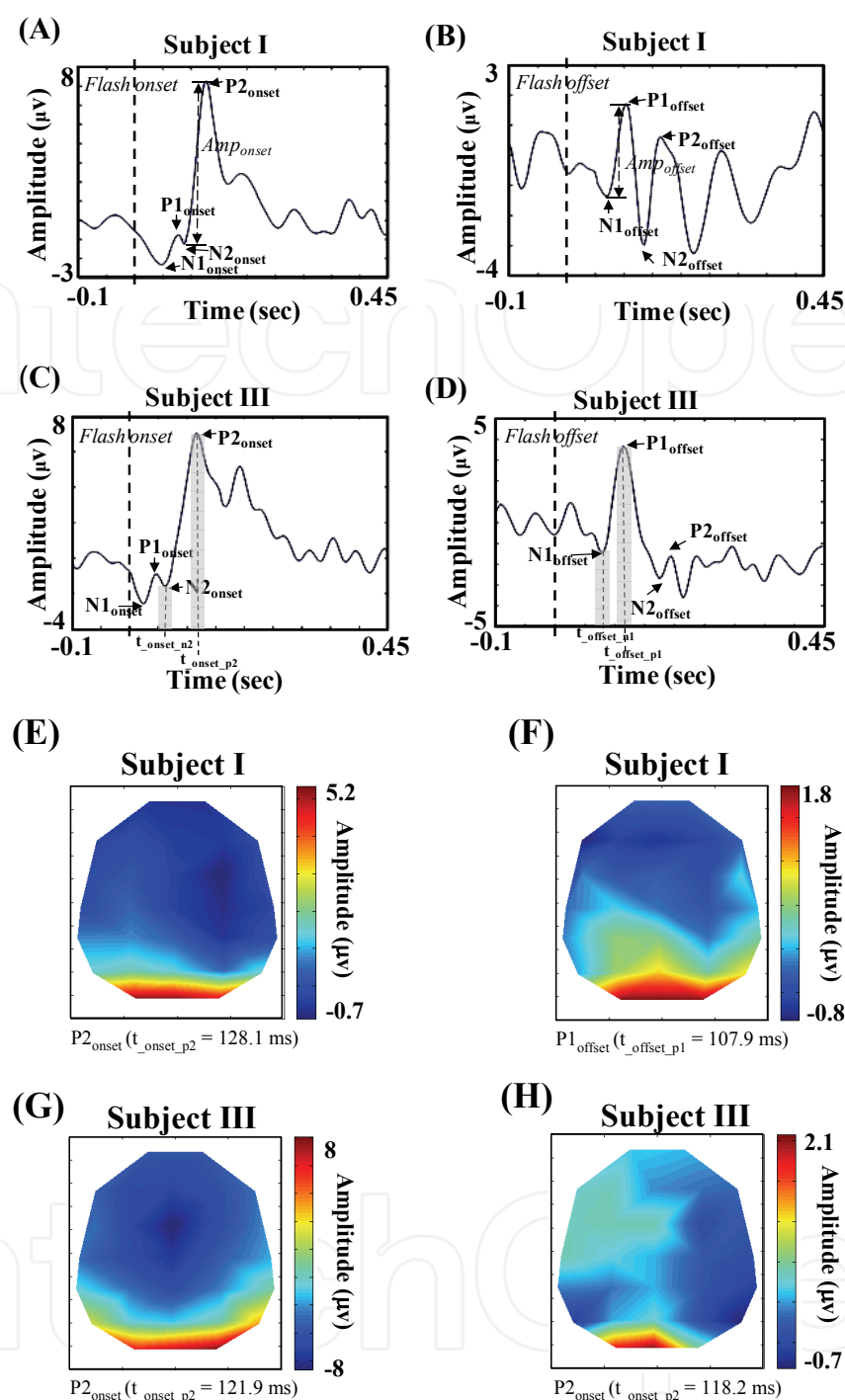


Fig. 2. Examples of the measured onset and offset FVEPs. Both the onset and offset FVEPs have two major negative and two positive peaks within 200 ms after flash onset and offset, termed as  $N1_{\text{onset}}$ ,  $P1_{\text{onset}}$ ,  $N2_{\text{onset}}$ , and  $P2_{\text{onset}}$  in onset FVEP and  $N1_{\text{offset}}$ ,  $P1_{\text{offset}}$ ,  $N2_{\text{offset}}$ , and  $P2_{\text{offset}}$  in offset FVEP, respectively, which are all marked by arrows. (A) the onset FVEP in subject I. (B) the offset FVEP in subject I. (C) the onset FVEP in subject III. (D) the offset FVEP of subject III. The shaded areas are the time windows used for searching  $N2_{\text{onset}}$ , and  $P2_{\text{onset}}$ ,  $N1_{\text{offset}}$ , and  $P1_{\text{offset}}$ . (E) the topography of  $P2_{\text{onset}}$  in subject I. (F) the topography of  $P1_{\text{offset}}$  in subject I. (G) the topography of  $P2_{\text{onset}}$  in subject III. (H) the topography of  $P1_{\text{offset}}$  in subject III.

**2.4 Determination of gazed target by detecting the largest  $Amp_{onset}+Amp_{offset}$  among the averaged responses of all flickering channels**

The EEG recordings at Oz were inevitably contaminated by peripheral onset and offset FVEPs induced from non-target visual stimuli. Since FVEPs are time-locked and phase-locked to the visual stimulus (Sutter, 1992), onset and offset FVEPs induced from the central visual field are synchronized to the flash onsets and offsets of the gazed flickering stimulus, respectively. Peripheral visual responses that are asynchronous to the flash onsets and offsets of central visual stimulus can be suppressed using a simple averaging process. By comparing the averaged onset and offset responses, the stimulus producing the onset and offset FVEPs with the largest peak-to-valley features was identified as the gazed target.

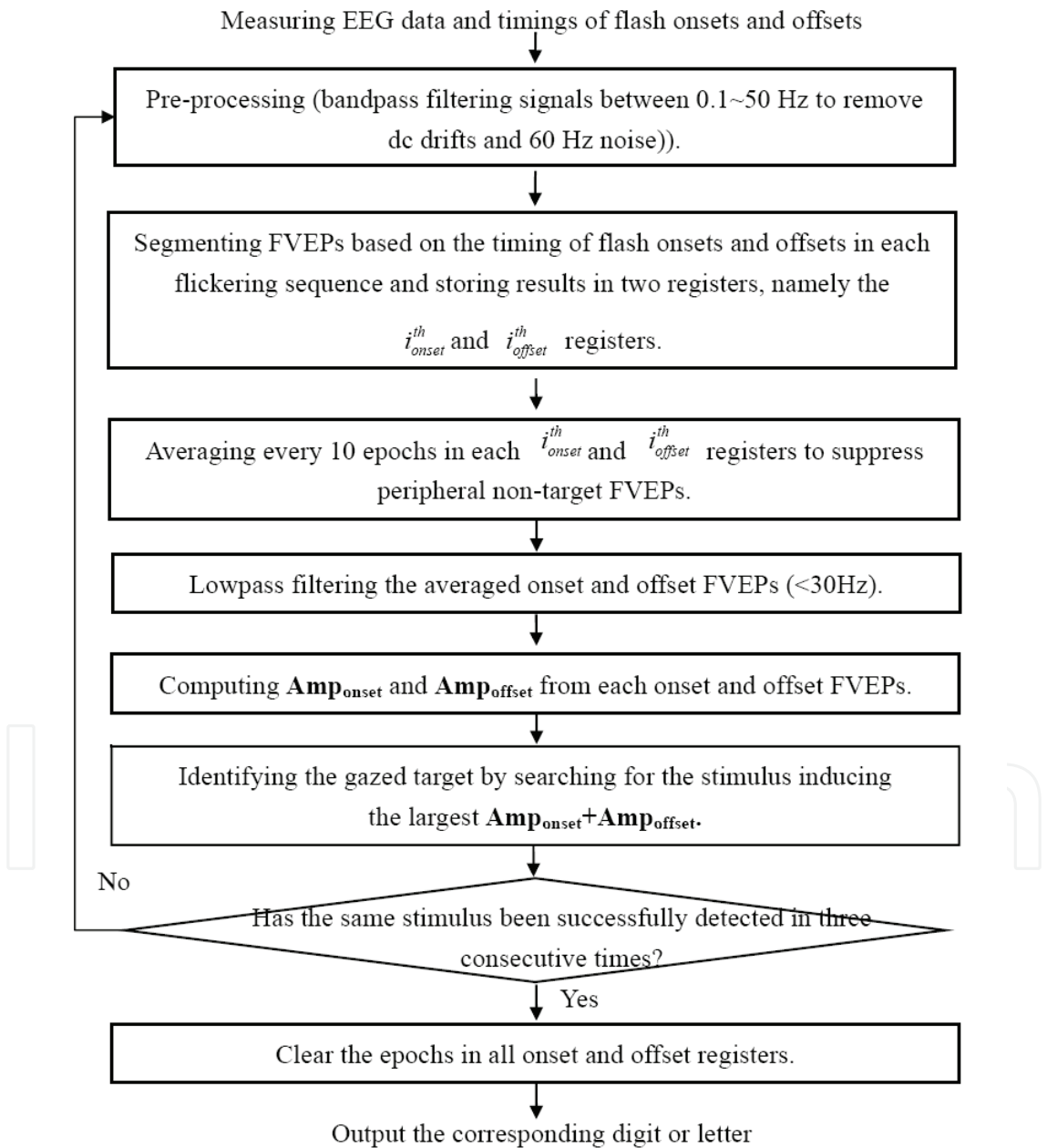


Fig. 3. The overall signal processing flow chart of the FVEP-based BCI system.



To suppress such interferences from non-target stimuli via averaging, the ON and OFF durations were designed to be random and all the flickering pattern sequences were generated in a manner that they were mutually independent. The Oz-EEG signals were segmented into epochs based on the flash onset or offset in the  $i$ th flickering sequences, i.e., from -0.1 to 0.45s, and stored in two computer registers, namely the  $i_{onset}^{th}$  and  $i_{offset}^{th}$  registers, respectively. To detect the gazed target, first, every  $N$  epochs ( $N=10$  in our implementation) in both  $i_{onset}^{th}$  and  $i_{offset}^{th}$  registers were averaged followed by lowpass (<30Hz) filtering (zero-phase, 6th-order, IIR Butterworth filter) to produce noise-suppressed onset and offset FVEPs. Second, the  $Amp_{onset}$  and  $Amp_{offset}$  induced from all flickering channels were computed. Third, the stimulus producing the largest  $Amp_{onset}+Amp_{offset}$  was recognized as the gazed target. Finally, the screen letter or digit representing the identified stimulus was sent out with a concurrent auditory bio-feedback presented to the subject, along with resetting the  $i_{onset}^{th}$  and  $i_{offset}^{th}$  registers. In our current design, a gazed stimulus was detected in every one second and was confirmed as the target after three consecutively successful detections, i.e., a letter or digit was sent out in every three seconds. The overall processing flowchart is summarized in Fig. 3.

### 3. Results

The primary advantage of current design of mutually independent flickering sequences is to enhance the visual responses arising from target stimuli while suppressing the interference from surrounding non-target flickering channels via averaging. Figure 4 illustrates the detection of largest  $Amp_{onset}$  and  $Amp_{offset}$  when one of subjects (subject I) was focusing binocularly on the stimulus FC-13 located at the center of the  $5 \times 5$  grid in the control study. The first panel shows the flickering sequences of stimulus FC-13 and the induced EEG signals at Oz, where the vertical solid and dashed lines indicates the flash onsets and offsets of flickering sequence FC-13, respectively. The Oz signals were segmented based on the flash onsets and offsets in the flickering sequence of stimulus FC-13 and the averaged results of every 10 consecutive segmented epochs were displayed in the panel labeled by FC-13 Onset and FC-13 Offset. Temporal waveforms in the remaining panels labeled by FC-j Onset and FC-j Offset,  $j = 1$  and 25, were generated in the same manner based on the flash onsets and offsets of flickering stimulus FC-j. Figure 5 provides another overall view of the averaged onset and offset FVEPs in which the location of each subplot corresponds to the location of associated stimulus. Since the central onset (or offset) FVEPs were time-locked and phase-locked to the flash onsets (or offsets) of the target flickering sequence but the peripheral FVEP epochs were asynchronized to such flash onsets (or offsets), the averaged onset and offset FVEPs induced from stimulus FC-13 exhibited the largest  $Amp_{onset}$  and  $Amp_{offset}$  after averaging and have been successfully segregated from the surrounding flickering sequences. Figure 6 shows that the 10-trial averaged onset and offset FVEPs provoked from stimulus FC-13 can only be recognized at O1, O2 and Oz channels in the occipital area, validating the use of single Oz channel in the application study.

To further assess the detection accuracy of using the onset and offset FVEPs, each subject was instructed to gaze binocularly at the center of each flickering channel for one-minute recording in the control study. The detection of gazed FC was performed one by one continuously until all of the twenty-five FCs were processed. Different numbers of epochs were averaged to compute the values of  $Amp_{onset}+Amp_{offset}$  for the subsequent estimation of

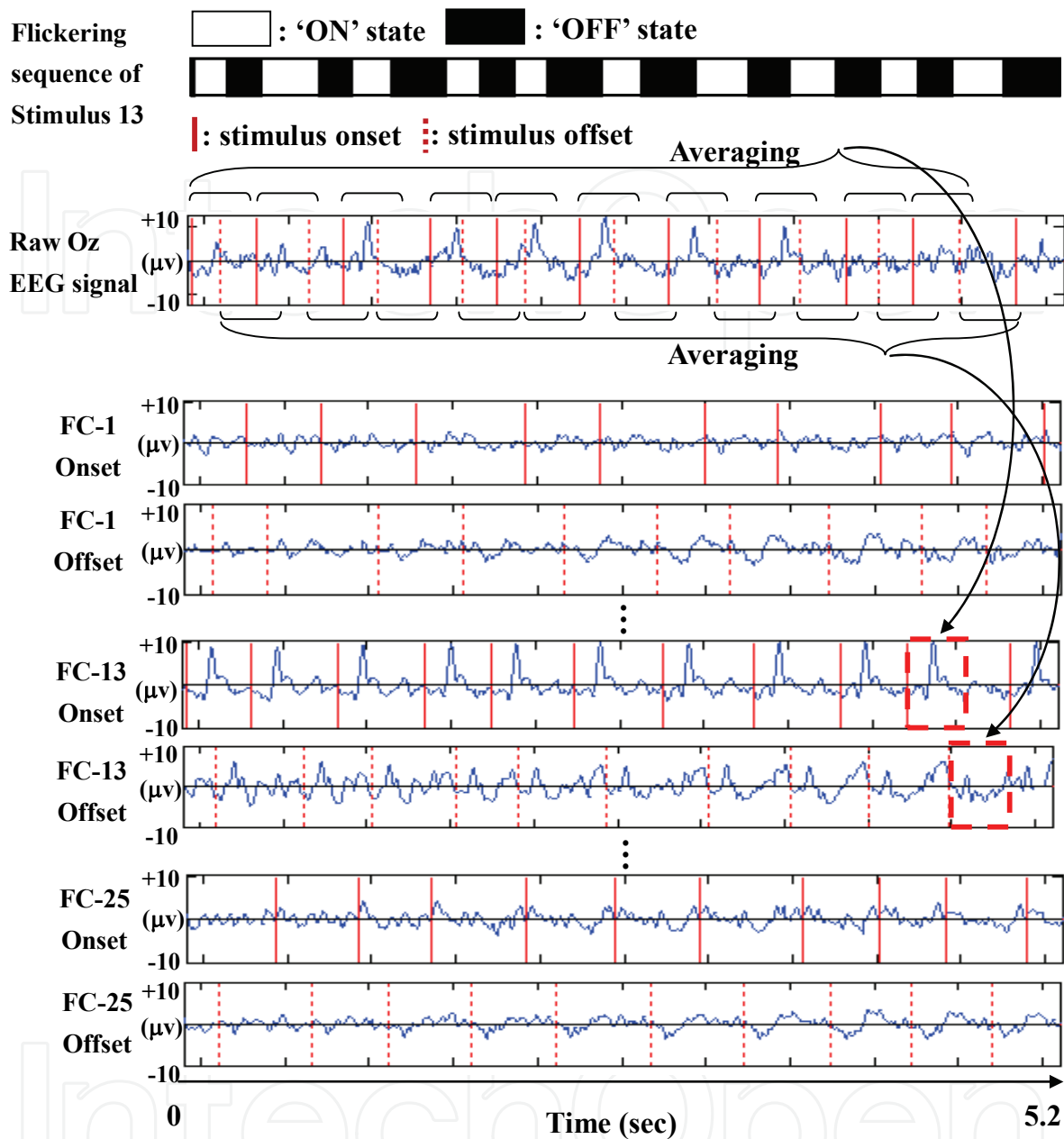


Fig. 4. Extraction of central onset and offset FVEPs when a subject stares at stimulus FC-13 in the control study. The first panel shows the flickering stimulus sequence, namely FC-13, where vertical solid and dashed marks denote the flash onsets and offsets, respectively. The Oz-EEG signals are segmented based on the flash onsets and offsets in stimulus FC-13 followed by averaging every 10 consecutive segmented epochs and results are displayed in the panel labeled by FC-13 Onset and FC-13 Offset. Temporal waveforms in the remaining panels labeled by FC-j Onset and FC-j Offset,  $j=1$  and 25, show the results generated in the same manner based on the flash onsets and offsets of flickering stimulus FC-j. The averaged onset and offset FVEPs induced from stimulus FC-13 exhibited the largest  $\text{Amp}_{\text{onset}}$  and  $\text{Amp}_{\text{offset}}$  so that FC-13 was identified as the target stimulus.

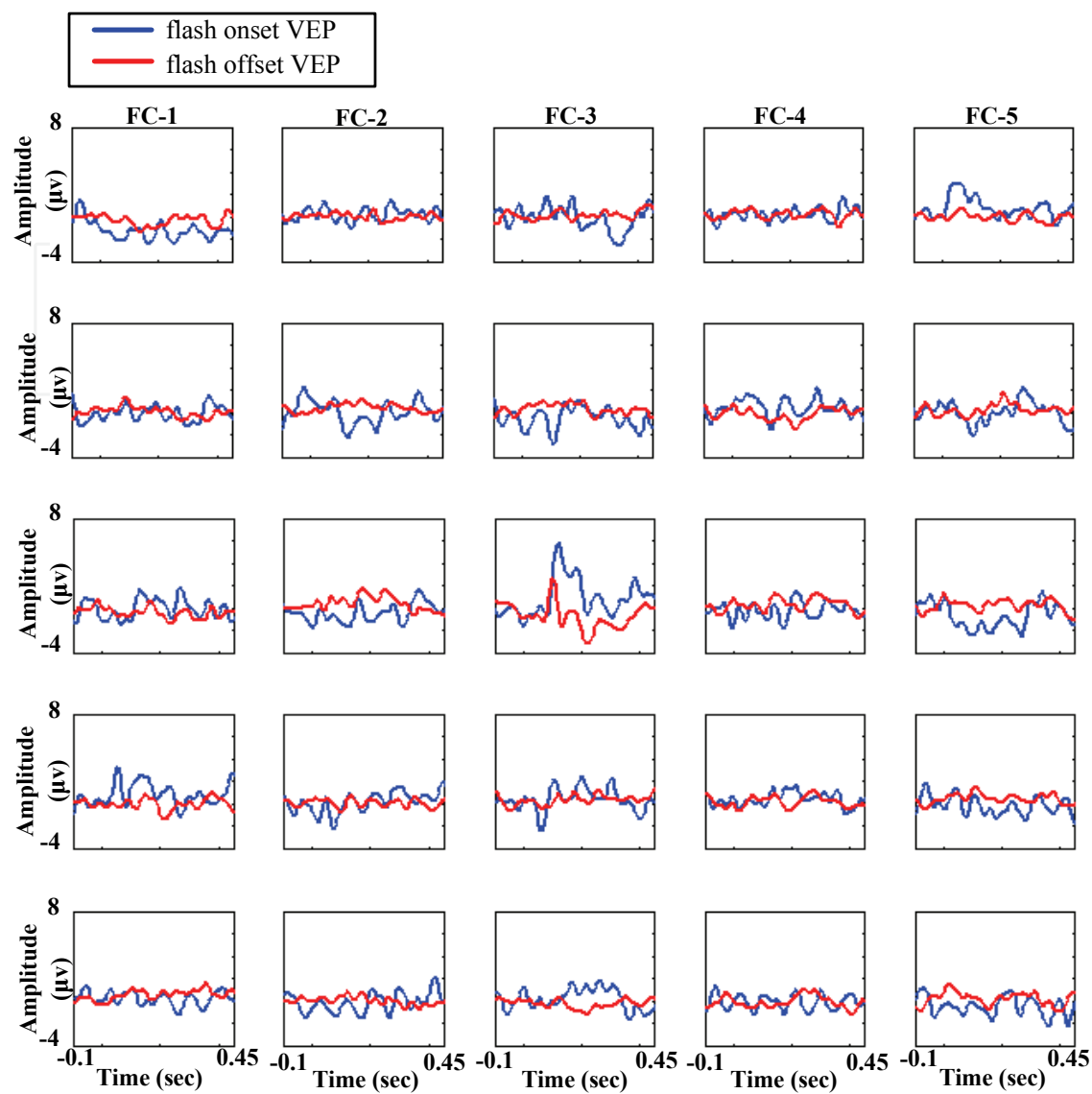


Fig. 5. Overall view of averaged central onset and offset FVEPs when a subject stares at stimulus FC-13 in the control study. Averaged onset (blue curve) and offset (red curve) FVEPS obtained from the procedure described in Fig. 3 are displayed in the subplots of a 5x5 array. Position of each subplot corresponds to the position of the stimulus used in the control study. The onset and offset FVEPs in the panel FC-13 shows the most prominent onset and offset FVEPs.

detection accuracy of gazed target, which was defined as the number of correct detections ( $N_{\text{correct}}$ ) divided by the total detection number ( $N_{\text{total}}$ ), i.e.,  $N_{\text{correct}}/N_{\text{total}}$ . Figure 7 depicts the mean detection accuracies over the five participants with 1, 5, 10, 15, 20, 25, 30, and 35 epochs being averaged using  $\text{Amp}_{\text{onset}}+\text{Amp}_{\text{offset}}$  (dashed curve) and  $\text{Amp}_{\text{onset}}$  (solid curve), respectively. The mean accuracies of using  $\text{Amp}_{\text{onset}}+\text{Amp}_{\text{offset}}$  were 31.8%, 73.8%, 97.4%, 99.5%, 100%, 100%, 100%, and 100%, respectively, in comparison with that of using  $\text{Amp}_{\text{onset}}$  which were 27.8%, 67.0%, 91.2%, 95.0 %, 95.8%, 99.0%, 99.4%, and 99.8%, respectively, and that of using  $\text{Amp}_{\text{offset}}$  which were 27.7%, 45.3%, 57.5%, 78.3%, 92.0%, 98.1%, 99.2%, and 99.5% (dotted curve), respectively. The resulting accuracies from each individual were further presented in Table 1A and 1B, respectively, where the accuracies of using

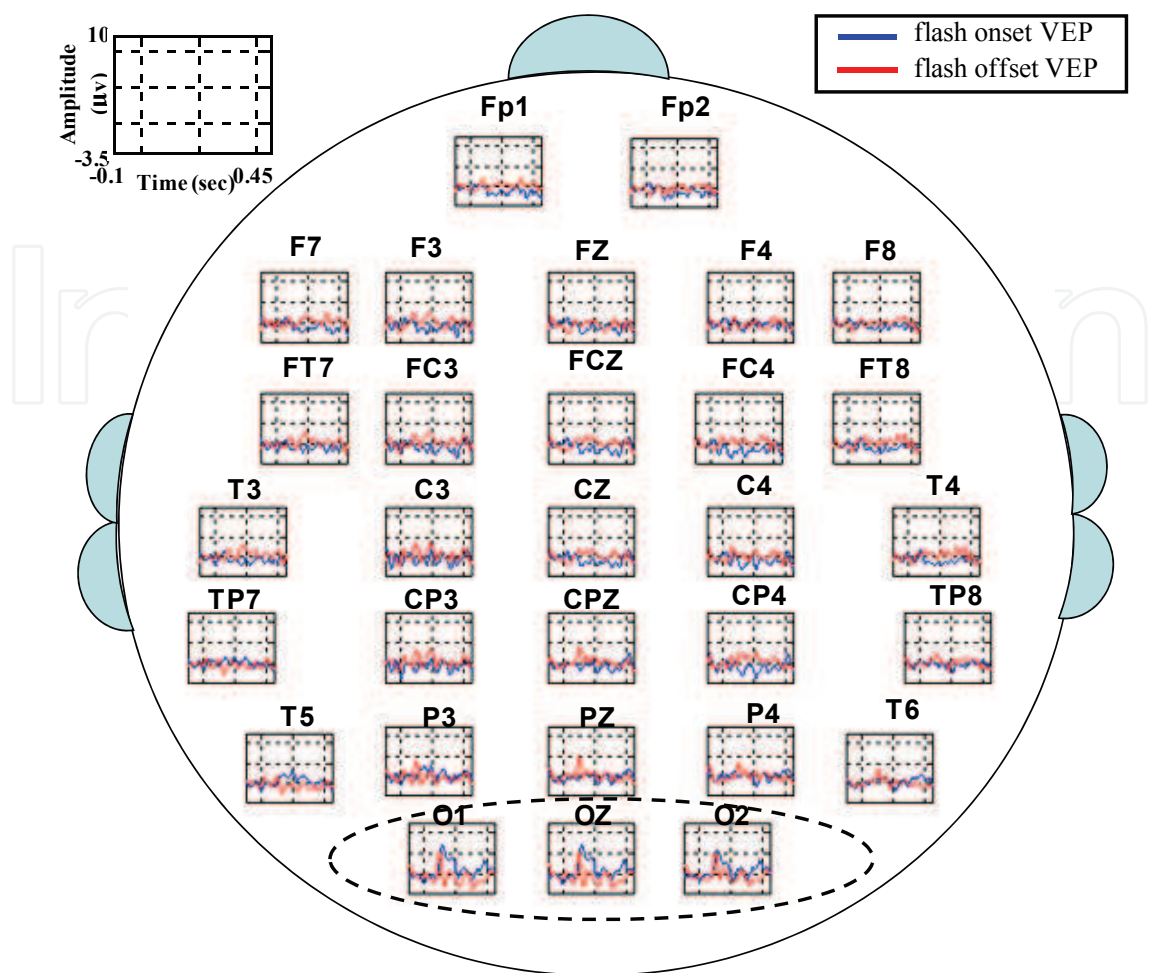


Fig. 6. Whole-head channel plot of ten-trial averaged FVEPs. The 10-trial averaged onset and offset FVEPs resulted from stimulus FC-13 can only be identified at O1, O2 and Oz channels in the occipital area, validating the use of single Oz channel in the application study.

$Amp_{onset} + Amp_{offset}$  with 10-epoch averages were significantly higher in comparison with that of using  $Amp_{onset}$  with 10-epoch averages (paired  $t$ -test,  $p < 0.05$ ), and reached 100% when 20 or more epochs were averaged. To compromise the computational efficiency and accuracy in the current BCI system, 10-epoch averages were adopted since accuracy higher than 95% has been achieved.

Averages and standard deviations of the latencies and amplitudes of the  $N2_{onset}$ ,  $P2_{onset}$ ,  $N1_{offset}$ , and  $P1_{offset}$  peaks induced from the twenty-five flickering channels for each subject in the control study were computed on the basis of 100 epochs (Table 2A and Table 2B). Results elucidated small variations (less than 5 ms) in the latencies of four featured peaks (Table 2A) as well as relative significance between  $Amp_{onset}$  and  $Amp_{offset}$ , where the mean value of  $Amp_{offset}$  ( $3.41\mu V$ ) over five subjects was about half (45.6%) of the mean value of  $Amp_{onset}$  ( $7.47\mu V$ ), suggesting the reliability of onset and offset FVEPs in the proposed FVEP-based BCI system. In addition, the short latencies (the longest one occurred at  $P2_{onset}$  peaks with 130 ms) endorse the feasibility of high communication rate.

In the application study, each subject was requested to produce a string '0287513694E'. The letter 'B' was not used in this experiment since it was used for the purpose of correcting erroneous spelling. By detecting the largest values of  $Amp_{onset} + Amp_{offset}$  among the

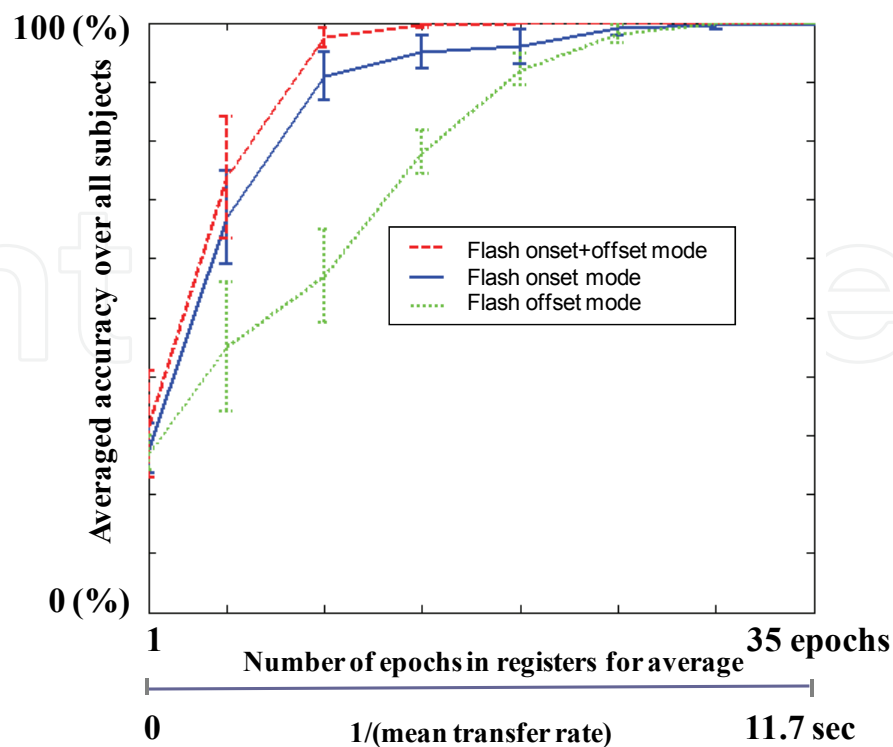


Fig. 7. Comparison of  $\text{Amp}_{\text{onset}} + \text{Amp}_{\text{offset}}$ ,  $\text{Amp}_{\text{onset}}$ , and  $\text{Amp}_{\text{offset}}$  detected accuracies. Five subjects with 1, 5, 10, 15, 20, 25, 30, and 35 averaged epochs are used for comparison. The mean accuracies of using  $\text{Amp}_{\text{onset}} + \text{Amp}_{\text{offset}}$  are 31.8%, 73.4%, 97.4%, 99.5%, 100%, 100%, 100%, and 100%, respectively, compared to that of using  $\text{Amp}_{\text{onset}}$  which are 27.8%, 67.0%, 91.2%, 95.0%, 95.8%, 99%, 99.4%, and 99.8%, respectively.

averaged responses of all flickering channels, the gazed FC was determined in every second by a personal computer (CPU 3.0 GHz/ 1GB RAM). Whenever each gazed digit or letter was confirmed for three consecutive times by the system, the subject was prompted by voice feedback to proceed with the next digit/letter. All five participants completed the string with minor errors, which were marked underlined. In addition to the accurate rate,  $N_{\text{correct}}/N_{\text{total}}$ , the command transfer interval (CTI) and information transfer rate per minute (ITR) were also computed. The command transfer interval, CTI, was defined as total experimental time ( $T_{\text{total}}$ ) divided by the number of total output digits and letters, i.e.,  $T_{\text{total}}/N_{\text{total}}$ . The information transfer rate per minute (ITR) was computed by

$$\frac{\text{Bits}}{\text{command}} = \log_2 N + P \log_2 P + (1 - P) \log_2 [(1 - P) / (N - 1)] \quad (1)$$

$$\text{ITR} = \frac{\text{Bits}}{\text{command}} \cdot \frac{60}{\text{CTI}} \quad (2)$$

where  $N$  is the total number of stimuli and  $P$  is the accuracy (Kelly et al., 2005). The mean accuracy of using  $\text{Amp}_{\text{onset}} + \text{Amp}_{\text{offset}}$  was 92.18 %, and the mean CTI and ITR were 5.52 sec/command and 33.65 bits/min, respectively.



All subjects who took part in this study have successfully completed a string (see Table 3A and 3B) with few errors either using the  $Amp_{onset}+Amp_{offset}$  or  $Amp_{onset}$ . Nevertheless, the familiarity of experiment and attention of subjects may affect the detection rates. In this study, two of the five subjects had one-hour training before this task while the other three were naïve subjects. We observed that the experienced subjects have better concentration on the target stimulus than the naïve subjects who were distracted occasionally by surrounding non-target stimuli. For example, subject IV has incautiously shifted his gaze on the wrong stimulus ‘7’ after selected ‘3’ (see Table 3). The experienced group (i.e., subject I and II) has performed superiorly with faster ITR (45.73 bits/min) and higher accuracy (100%) than the naïve group from which the ITR and accuracy were 25.06 bit/min and 86.07%, respectively.

(A) Results of using  $Amp_{onset}+Amp_{offset}$

Subject	Number of epochs for averaging							
	1	5	10	15	20	25	30	35
I	30%	88%	98%	100%	100%	100%	100%	100%
II	23%	66%	97%	99%	100%	100%	100%	100%
III	31%	79%	98%	100%	100%	100%	100%	100%
IV	28%	62%	95%	99%	100%	100%	100%	100%
V	47%	74%	99%	100%	100%	100%	100%	100%
Average	31.8%	73.8%	97.4%	99.5%	100%	100%	100%	100%

(B) Results of using  $Amp_{onset}$

Subject	Number of epochs for averaging							
	1	5	10	15	20	25	30	35
I	33%	76%	91%	97%	98%	99%	100%	100%
II	24%	63%	85%	90%	91%	97%	98%	99%
III	32%	74%	94%	96%	97%	100%	100%	100%
IV	25%	65%	93%	96%	97%	100%	100%	100%
V	25%	57%	93%	95%	96%	99%	99%	100%
Average	27.8%	67.0%	91.2%	95.0%	95.8%	99.0%	99.4%	99.8%

Table 1. Comparison of the results using  $Amp_{onset}+Amp_{offset}$  and  $Amp_{onset}$ .

(A) Latencies of onset and offset FVEP features.

Subject	Onset FVEP		Offset FVEP	
	N2 <sub>onset</sub>	P2 <sub>onset</sub>	N1 <sub>offset</sub>	P1 <sub>offset</sub>
I	95.5±3.45	127.8±2.38	75.2±3.83	108.3±3.21
II	82.3±3.29	125.2±3.21	72.2±4.19	109.3±4.22
III	74.1±2.13	121.3±2.55	81.8±3.81	118.7±2.25
IV	78.2±3.71	118.9±2.53	78.6±3.14	112.1±4.91
V	92.6±1.75	123.4±3.01	72.9±2.11	120.4±3.62
Average	84.5±8.71	123.3±4.16	72.2±5.29	113.68±5.90

(B) Amplitudes of onset and offset FVEP features.

Subject	Onset FVEP		Offset FVEP	
	N2 <sub>onset</sub>	P2 <sub>onset</sub>	N1 <sub>offset</sub>	P1 <sub>offset</sub>
I	-1.13±0.77	7.20±1.13	-1.35±0.55	1.68±0.74
II	-2.08±1.05	4.69±1.54	-1.12±0.45	1.34±0.51
III	-3.24±0.68	7.19±1.16	-1.47±0.93	3.74±0.93
IV	-2.20±0.56	1.67±0.62	-0.41±0.25	1.84±0.67
V	-1.34±0.48	6.66±0.54	-1.89±0.48	2.21±0.57
Average	-1.99±0.72	5.48±2.18	-1.25±0.64	2.16±0.93
Average	Amp <sub>onset</sub> =7.47±2.47		Amp <sub>offset</sub> =3.41±1.01	

Table 2. The latencies and amplitudes of the N2<sub>onset</sub>, P2<sub>onset</sub>, N1<sub>offset</sub>, and P1<sub>offset</sub> peaks induced from the 25 flickering channels.

Subject	Input results (wrong underlined)	Total time (sec)	Accuracy (N <sub>correct</sub> /N <sub>total</sub> )	CTI (sec/command)	ITR (bits/min)
I	0287513694E	48	11/11 (100%)	4.36	49.26
II	0287513694E	56	11/11 (100%)	5.09	42.20
III	028751236794E	81	11/13 (84.6%)	6.23	23.08
IV	02875137694E	70	11/12 (91.7%)	5.83	29.69
V	027875136934E	79	11/13 (84.6%)	6.07	24.04
Average		66.8	92.18%	5.52	33.65

Table 3. Results of producing the string ‘0287513694E’ from five subjects.

4. Discussion

FVEP has been a popular clinical index to monitor anesthesia level during surgery (Raitta et al., 1979; Uhl et al., 1980), to diagnose prechiasmal and retrochiasmal lesions (Carlin et al.,

1983; Kriss et al., 1982; Markand et al., 1982; Wilson, 1978), to indicate intracranial pressure induced by head injury (McSherry et al., 1982), and to alarm brain death (Reilly et al., 1978; Trojaborg & Jorgensen 1973). FVEP can be measured in patients who have very poor visual acuity (Spehlmann, 1985), and some studies also reported that the FVEP can be measured in patients who can see flashes clearly but not pattern stimuli owing to their partial deficiencies in optical fiber connections between retina and visual cortex (Kriss et al., 1982; Wilson, 1978). These studies suggest that the FVEP is a widely measurable biosignal which has also been used as a control signal for BCI systems (Lee et al., 2005; Lee et al., 2006; Sutter, 1992).

The visual 'Flash offset' responses have been investigated in the single-neuron recording (Duysens et al., 1996; Brooks & Huber, 1972) and electroretinogram (ERG) (Kondo et al., 1998) studies. It has been reported that at least one-third of the cortical cells in visual area (area 17 and 18) produced the visual 'Flash offset' responses that were sensitive to the duration of preceding light stimulus (Duysens et al., 1996). In particular, the amplitudes of such visual 'Flash offset' responses were proportional to the duration of preceding light stimuli (Duysens et al., 1996; Brooks & Huber, 1972). In our study, the visual 'Flash offset' responses were not only clearly observed (Fig. 5), but also preserved the characteristics of central magnification similar to onset FVEP, which was in line with the Duysens et al.'s results in which the presence of offset-FVEP central magnification in offset FVEP was suggested to be generated at cortical level rather than the input from the Y-OFF cells in LGN (Duysens et al., 1996), since the visual 'Flash offset' responses from Y-OFF cells in LGN should be specially prominent with peripheral fields (Ferster, 1990). Duysens et al. (1996) further pointed out that the visual 'offset' response was duration-dependent which may be caused by "cortical disinhibition", meaning a release from the inhibition of other surrounding cortical cells over the same region after long-duration light stimulation.

The flickering sequences in this study were generated by random ON and OFF durations. Each ON or OFF state in the flickering sequence was a concatenation of one fixed length (116.7 ms) and a variable length (uniformly distributed between 0 ms and 233.3 ms). The fixed duration was designed to prevent the major visual response of current onset or offset FVEP overlapped with the incoming offset or onset FVEP, and the random duration was used to generate temporal independence among different flickering sequences. The ensemble average FVEPs evoked by flash onsets (or offsets) can be viewed as sums of two stimulus-driven responses: the time-locked FVEPs induced from the target flickering sequence and the non-time-locked visual responses from other flickering sequences. The same ensemble averaging process also attenuates noise, random VEPs and the endogenous EEG. In order to further examine the uncorrelation among different flickering sequences, the correlation coefficients between any two flickering sequences with different temporal lengths ( $N$ ), from 1000 frames to 100000 frames, were computed. The formula of correlation

coefficient is given by  $Coef(X, Y) = \frac{E[(X - \bar{X}) \cdot (Y - \bar{Y})]}{(E[(X - \bar{X})^2])^{1/2} \cdot (E[(Y - \bar{Y})^2])^{1/2}}$ , where  $E[\cdot]$  represents

the operator of expected value,  $X$  and  $Y$  are two different flickering sequences, and  $\bar{X}$  and  $\bar{Y}$  are the mean (expected) values of  $X$  and  $Y$ , respectively. For pairs of flickering stimulus sequences of lengths 1000, 10000, 20000, 30000, 40000, 50000, 60000, 70000, 80000, 90000, and 100000, we tested the hypothesis that the mean correlation coefficient between any two sequences was greater than  $r_c$ , where  $r_c$  is the critical value of  $Coef(X, Y)$  for a one-tailed test with  $p < .01$  (e.g.,  $r_c$  value is 0.0734 for stimulus sequence of lengths 1000). In every case, we rejected the hypothesis that the observed  $Coef(X, Y)$  exceeded  $r_c$ .

The mean ITR (33.65 bits/min) and accuracy (92.18%) of the proposed BCI can be further improved in the following two ways. First, advanced signal processing techniques can be applied to extract the FVEPs with higher SNR so that much fewer epochs are used in the averaging process for suppressing peripheral visual responses. For example, the independent component analysis (ICA) (Hyvarinen & Oja, 1997) can be used to extract the FVEP in a single trial (Lee et al., 2003; Jung et al., 2001; Tang et al., 2002). Since the FVEP is time-locked and phase-locked, the gaze-FC can be identified by examining the latencies of central FVEP and thereby higher ITR may be achieved with few averaged epochs. Second, effective classifiers, such as artificial neural network (ANN) (Haselsteiner & Pfurtscheller, 2000; Palaniappan et al., 2002), support vector machine (SVM) (Meinicke et al., 2003) and linear discriminate analysis (LDA) (Donchin et al., 2000; Hinterberger et al., 2003) can be adopted for accuracy improvement. Cheng et al. (2006) have improved the mean ITR of their SSVEP-based BCI from 27.15 bits/min to 43 bits/min by designing an optimal bipolar measurement with the use of ICA. Meinicke et al. (2003) took the advantage of SVM and have increased the mean ITR of their P300-based BCI from 12 bits/min to 50.5 bits/min. Based on the ICA and advanced classifiers, the performance improvement of our BCI system can be expected.

Comparing the proposed FVEP-based BCI system with other SSVEP-based (including the gaze-dependent SSVEP and attention-regulated SSVEP) or FMFVEP-based systems, both the flickering design and the translation algorithm in these three categories are different. In our system, mutually independent flickering sequences were designed to induce onset and offset FVEPs and the temporally-encoded stimulus onsets and offsets were used to segment FVEPs followed by averaging and comparison for the detection of gazed stimulus. In contrast, the SSVEP-based system was a frequency-encoded method which encoded flickering sequences in distinct frequencies, that is, each visual stimulus was designed to have its own flickering frequency, and the gazed target was identified by finding the stimulus that contributed maximum power of SSVEP at Fourier spectrum. In the FMFVEP-based system, it presumed identical response of FVEP across all trials and used such an "expected response" as the template in correlation computation (Sutter, 1992). The flickering sequence that produced the maximal correlation was determined as the target stimulus. Of note is that the computational complexities for SSVEP system and FMFVEP system were orders of  $M \cdot \log_2 M$  ( $M=512$ ) and  $M^2$  ( $M=300$ , at 250 Hz sampling rate and 10/sec flickering activation rate), respectively, where  $M$  was number of data points in data processing. By taking the advantage of the design of mutually independent random sequences, the proposed system only requires simple averaging, leading to computation complexity no larger than order of  $N$  ( $N=10$ ), where  $N$  is the number of epoch used in averaging.

The proposed study utilizes focal stimulus light to induce cortical FVEPs. Intraocular light scattered in ocular media and reflected from ocular surfaces may evoke photoreceptors on peripheral visual fields and induce stray light responses (Sandberg et al., 1996; Shimada & Horiguchi, 2003; Stenbacka & Vanni, 2007), which are mainly contributed from rod cells owing to their nondirectional sensitivity (Sandberg et al., 1996). Since the stray light responses are induced by the light which has been reflected and nondirectionally scattered for multiple times, the stray light responses have delayed and weaker responses compared to those evoked from fovea region (Sandberg et al., 1996; Shimada & Horiguchi, 2003). Nevertheless, in this study, the stray light responses are not clearly observed (see Fig. 2, 4 and 5). Possible reasons are as follows. First, the data were recorded in a dimly illuminated room instead of a completely dark environment so that the sensitivity of peripheral

photoreceptors to stray light is reduced (Stenbacka & Vanni, 2007). Second, our study utilizes multiple flickering stimuli presented simultaneously on a screen. The flickering states of each FC are determined by a self-generated random function and independent of the flickering of other FCs. Due to the property of mutual independence among different FCs, it keeps approximately half of FCs in ON state and the other half of FCs in OFF states which results in no large change in net luminance modulation and the stray light in the periphery is not largely modulated (Riemsdag et al., 1985; Fry & Bartley, 1935). Third, since the interferences of FVEP from non-gazed FC have been successfully suppressed using averaging technique in this study and the responses of stray light from peripheral visual fields are usually delayed and weaker than FVEPs induced from central visual fields, we can speculate that the interference of stray light responses induced from non-gazed FCs can be suppressed as well after applying the averaging process. However, the responses of the visual system are dependent on spatial and temporal parameters, such that periphery may sometimes dominate the central response even when the stimuli are central in some practical applications. The issues of precise contribution from periphery are beyond the scope of current study and will be investigated in future work.

It is noted that operations of both the gaze-dependent VEP-based BCI system and the popular eye tracker systems are associated with eye motions. Eye tracking systems require constant light sources, such as infrared light, and a stationary environment with tolerance of minor head movements (Duchowski, 2003). Although eye trackers have been well-developed, some physiological or spatial calibration issues still limit its applications in practical use. First, eye trackers are operated based on image analysis to detect retro-reflectivity of two reference points, e.g., reflection from pupil center and the corneal of a stationary light source. As a consequence, eye tracking systems require stationary environments to prevent influence of glint from surrounding false objects (Duchowski, 2003). Second, available visual angles for eye tracking systems are usually operating within  $\pm 45^\circ$  so that the boundaries of iris or cornea can be well captured. Third, the velocities of eye saccade can be up to  $700^\circ/\text{sec}$  within a duration as short as 20ms (Carpenter, 1988), and thereby most video-based eye trackers are equipped with costly high-speed video capture systems ( $>250\text{ Hz}$ ) (Duchowski, 2003). In contrast, the VEP-based BCI aims to develop a user-friendly and low-cost system but with the compromised response time of  $1 \sim 4$  seconds (Cheng et al., 2002; Cheng et al., 2006; Kelly et al., 2005; Lee et al., 2005; Lee et al., 2006; Middendorf et al., 2000; Sutter 1992; Trejo et al., 2006), which requires only an EEG and an EOG channels.

## 5. Conclusion

In this study, a gaze-dependent FVEP-based BCI with ITR of 33.65 bits/min has been proposed. Subjects can shift their gazes at target flashing digits or letters to generate a string for communication purposes. The salient features of the proposed system include (1) FVEP is a reliable neuroelectric signal with fast response that can be used to achieve high ITR, (2) mutually random sequences are designed to suppress inter-flickering-channel interferences via simple averaging which is suitable for real-time processing, (3) the mutually independent sequences consisting of ON and OFF states can be used to induce onset and offset FVEPs at the timing of stimulus onsets and offsets for increasing the detection rates of gazed stimulus, (4) the central magnification of offset FVEP was confirmed in this study and has been used to incorporate with onset FVEP for defining more reliable feature



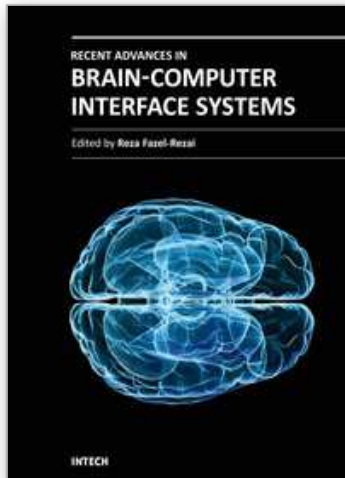
$Amp_{onset} + Amp_{offset}$  in identifying gazed stimulus, (5) the mean ITR using  $Amp_{onset} + Amp_{offset}$  achieves 33.65 bits/min, which is higher than the maximum ITR (~25 bits/min) in classical BCI systems (Walpow et al., 2002), with satisfactory mean detection rate 92.18%

## 6. References

- Birbaumer, N.; Flor, H.; Ghanayim, N.; Hinterberger, T.; Iverson, I.; Taub, E.; Kotchoubey, B.; Kubler, A. & Perelmouter, J. (1999). A spelling device for the paralyzed. *Nature*, Vol. 398, 297 – 298.
- Blankertz, B.; Dornhege, G.; Krauledat, M.; Muller, K. R. & Curio, G. (2007). The non-invasive Berlin brain- computer interface: fast acquisition of effective performance in untrained subjects. *NeuroImage*, Vol. 37, No. 2, 539-550.
- Brooks, B. & Huber, C. (1972). Evidence for the role of the transient neural “off-response” in perception of light decrement. A psychophysical test derived from neuronal data in the cat. *Vision Research*, Vol. 12, No. 7, 1291-1296.
- Carlin, L.; Roach, E. S.; Riela, A.; Spudis, E. & McLean, W. T. (1983). Juvenile metachromatic leukodystrophy: Evoked potentials and computed tomography. *Annals of Neurology*, Vol. 13, No. 1, 105-106.
- Carpenter, R. H. S. (1988). *Movements of the eyes, 2nd edition*, Pion, ISBN 9780850861099, London.
- Cheng, M.; Gao, X.; Gao, S. & Xu, D. (2002). Design and implementation of a brain-computer interface with high transfer rates. *IEEE Transactions on Biomedical Engineering*, Vol. 49, No. 10, 1181-1186.
- Donchin, E.; Spencer, K. M. & Wilesinghe, R. (2000). The mental prosthesis: Assessing the speed of a P300-based braincomputer interface. *IEEE Transactions on Rehabilitation Engineering*, Vol. 8, No. 2, 174 – 179.
- Duchowski, A. T. (2003). *Eye tracking methodology: theory and practice*. Springer-Verlag, ISBN 978-1846286087, London.
- Duysens, L.; Orban, G. A.; Cremieux, J. & Maes, H. (1985). Visual cortical correlates of visible persistence. *Vision Research*, Vol. 25, No. 2, 171-178.
- Duysens, L.; Maes, H. & Orban, G. A. (1987). The velocity dependence of direction selectivity of visual cortical neurones in the cat. *Journal of Physiology*, Vol. 387, June, 95-113.
- Duysens, J.; Schaafsma, S. J. & Orban, G. A. (1996). Cortical off response tuning for stimulus duration. *Vision Research*, Vol. 36, No. 20, 3243-3251.
- Ferster, D. (1988). Spatially opponent excitation and inhibition in simple cells of the cat visual cortex. *Journal of Neuroscience*, Vol. 8, 1172-1180.
- Fisch, B. J. & Spehlmann, R. (1999). Spatial analysis of the EEG. In: *Fisch and Spehlmann's EEG primer: basic principles of digital and analog EEG.*, Fisch, B. J., 73-92, Elsevier, ISBN 9780444821485, Amsterdam.
- Fry, G. A. & Bartley, S. H. (1935). The relation of stray light in the eye to the retinal action potential. *The American Journal of Physiology*, Vol. 111, 335-340.
- Haselsteiner, E. & Pfurtscheller, G. (2000). Using time-dependent neural networks for EEG classification. *IEEE Transactions on Rehabilitation Engineering*, Vol. 8, No. 4, 457-463.
- Hyvarinen, A. & Oja, E. (1997). A fast fixed-point algorithm for independent component analysis. *Neural Computing*, Vol. 9, No. 7, 1483-1492.
- Jung, T. P.; Makeig, S.; Westerfield, M.; Townsend, J.; Courchesne, E. & Sejnowski, J. T. (2001). Analysis and visualization of single-trial event-related potentials. *Human Brain Mapping*, Vol. 14, No. 3, 166-185.

- Kelly, S. P.; Lalor, E. C.; Reilly, R. B. & Foxe, J. J. (2005). Visual spatial attention tracking using high density SSVEP data for independent brain-computer communication. *IEEE Transactions on Neural Systems and Rehabilitation Engineering*, Vol. 13, No. 2, 172-178.
- Hinterberger, T.; Kubler, A.; Kaiser, J.; Neumann, N. & Birbaumer, N. (2003). A brain-computer interface (BCI) for the locked-in: comparison of different EEG classifications for thought translation device. *Clinical Neurophysiology*, Vol. 114, No. 3, 416-425.
- Kondo, M.; Miyake, Y.; Horiguchi, M.; Suzuki, S. & Tanikawa, A. (1998). Recording multifocal electroretinogram on and off responses in humans. *Investigative Ophthalmology & Visual science*, Vol. 39, No. 3, 574-580.
- Kriss, A.; Carroll, W. M.; Blumhardt, L. D. & Halliday, A. M. (1982). Pattern and flash evoked potential changes in toxic (nutritional) optic neuropathy. *Advances in Neurology*, Vol. 32, 11-19.
- Lee, P. L.; Wu, Y. T.; Chen, L. F.; Chen, Y.S; Cheng, C. M.; Yeh, T. C.; Ho, L. T.; Chang, M. S. & Hsieh, J. C. (2003). ICA-based spatiotemporal approach for single-trial analysis of postmovement MEG beta synchronization. *Neuroimage*, Vol. 20, No. 4, 2010-2030.
- Lee, P. L.; Wu, C. H.; Wu, Y. T.; Chen, L. F.; Yeh, T. C. & Hsieh, J. C. (2005). Visual evoked potential (VEP) - actuated brain computer interface: A brain-actuated cursor system. *Electronics Letters*, Vol. 21, No. 15, 832-834.
- Lee, P. L., Hsieh, J. C.; Wu, C. H.; Yeh, T. C. & Wu, Y. T. (2006) The brain computer interface using flash visual evoked potential and independent component analysis. *Annals of Biomedical Engineering*, Vol. 34, No. 10, 1641-1654.
- Markand, O. N.; Garg, B. P.; DeMyer, W. E. & Warren, C. (1982). Brain stem auditory, visual and somatosensory evoked potentials in leukodystrophies. *Electroencephalography and Clinical Neurophysiology*, Vol. 54, No. 1, 39-48.
- Mason, S. G. & Birch, G. E. (2000). A brain-controlled switch for asynchronous control applications. *IEEE Transactions on Biomedical Engineering*, Vol. 47, No. 10, 1297 - 1307.
- McSherry, J. W.; Walters, C. L. & Horbar, J. D. (1982). Acute visual evoked potential changes in hydrocephalus. *Electroencephalography and Clinical Neurophysiology*, Vol. 53, No. 3, 331-333.
- Meinicke, P.; Kaper, M.; Hoppe, F.; Heumann, M. & Ritter, H. (2003). Improving transfer rates in brain computer interfacing: a case study. *Advances In Neural Information Processing Systems*, Vol. 15, 1131-1138.
- Middendorf, M.; McMillan, G.; Calhoun, G. & Jones, K. S. (2000). Brain-computer interface based on the steady-state visual-evoked response. *IEEE Transactions on Rehabilitation Engineering*, Vol. 8, No. 2, 211-214.
- Muller-Putz, G. R.; Scherer, R.; Neuper, C. & Pfurtscheller, G. (2006). Steady-state somatosensory evoked potentials: suitable brain signals for brain-computer interface? *IEEE Transactions on Neural Systems and Rehabilitation Engineering*, Vol. 14, No. 1, 30-37.
- Odom, J. V.; Bach, M.; Barber, C.; Brigell, M.; Marmor, M. F.; Tormene, A. P.; Holder, G. E. & Vaegan. (2004). Visual evoked potentials standard. *Documenta Ophthalmologica*, Vol. 108, 115 - 123.
- Palaniappan, R.; Paramesran, R.; Nishida, S. & Saiwaki, N. (2002). A new brain-computer interface design using fuzzy ARTMAP. *IEEE Transactions on Neural Systems and Rehabilitation Engineering*, Vol. 10, No. 3, 140-148.

- Pfurtscheller, G.; Neuper, C.; Guger, C.; Harkam, W.; Ramoser, H.; Schlogl, A.; Obermaier, B. & Pgegenzer, M. (2000). Current trends in Graz brain-computer interface (BCI) research. *IEEE Transactions on Rehabilitation Engineering*, Vol. 8, No. 2, 216-219.
- Raitta, C.; Karhunene, U.; Seppalainen, A. M. & Naukkarinen, M. (1979). Changes in the electroretinogram and visual evoked potentials during general anaesthesia. *Graefes Archive for Clinical and Experimental Ophthalmology*, Vol. 211, No. 6, 139-144.
- Reilly, E. L.; Kondo, C.; Brunberg, J. A. & Doty, D. B. (1978). Visual evoked potentials during hypothermia and prolonged circulatory arrest. *Electroencephalography and Clinical Neurophysiology*, Vol. 45, No. 1, 100-106.
- Riemslog, F.C.; Ringo, J.L.; Spekreijse, H. & Verduyn Lunel, H.F. (1985). The luminance origin of the pattern electroretinogram in man. *Journal of Physiology*, Vol. 363, June, 191-209.
- Salmelin, R. & Hari, R. (1994). Characterization of spontaneous MEG rhythms in healthy adults. *Electroencephalography and Clinical Neurophysiology*, Vol. 91, No. 4, 237-248.
- Sandberg, M.A.; Pawlyk, B.S & Berson, E.L. (1996). Isolation of focal rod electroretinograms from the dark-adapted human eye. *Investigative ophthalmology and visual science*, Vol. 37, No. 5, 930-934.
- Shimada, Y. & Horiguchi, M. (2003). Stray light – induced multifocal electroretinograms. *Investigative ophthalmology and visual science*, Vol. 44, 1245-1251.
- Spehlmann, R. (1985). The transient VEP to diffuse light stimuli. In: *Evoked potential primer*, Spehlmann, R., 135-142, Butterworth Heinemann, ISBN 0750673338, Stoneham.
- Stenbacka, L. & Vanni, S. (2007). Central luminance flicker can activate peripheral retinotopic representation. *Neuroimage*, Vol. 34, No. 1, 342-348.
- Sutter, E.E. (1992). The brain response interface: communication through visually-induced electrical brain responses. *Journal of Microcomputer Applications*, Vol. 15, No. 1, 31-45.
- Tang, A.C.; Pearlmutter, B.A.; Malaszenko, N.A. & Phung, D.B. (2002). Independent components of magnetoencephalography: single-trial response onset times. *Neuroimage*, Vol. 17, No. 4, 1773-1789.
- Trejo, L.J.; Rosipal, R. & Matthews, B. (2006). Brain-computer interfaces for 1-D and 2-D cursor control: designs using volitional control of the EEG spectrum or steady-state visual evoked potentials. *IEEE Transactions on Neural Systems and Rehabilitation Engineering*, Vol. 14, No. 2, 225-229.
- Trojaborg, W. & Jorgensen, E.O. (1973). Evoked cortical potentials in patients with "isoelectric" EEGs. *Electroencephalography and Clinical Neurophysiology*, Vol. 35, No. 3, 301-309.
- Uhl, R.R.; Squires, K.C.; Bruce, D.L. & Starr, A. (1980). Effect of halothane anesthesia on the human cortical visual evoked response. *Anesthesiology*, Vol. 53, No. 4, 273-276.
- Wang, Y.; Wang, R.; Gao, X.; Hong, B. & Gao, S. (2006). A practical VEP-based brain-computer interface. *IEEE Transactions on Neural Systems and Rehabilitation Engineering*, Vol. 14, No. 2, 234-240.
- Wilson, W.B. (1978). Visual-evoked response differentiation of ischemic optic neuritis from the optic neuritis of multiple sclerosis. *American journal of ophthalmology*, Vol. 86, No. 4, 530-535.
- Wolpaw, J.R.; Birbaumer, N.; McFarland, D.J.; Pfurtscheller, G. & Vaughan, T.M. Brain-computer interfaces for communication and control. *Clinical Neurophysiology*, Vol. 113, No. 6, 767-791.



## **Recent Advances in Brain-Computer Interface Systems**

Edited by Prof. Reza Fazel

ISBN 978-953-307-175-6

Hard cover, 222 pages

**Publisher** InTech

**Published online** 04, February, 2011

**Published in print edition** February, 2011

Brain Computer Interface (BCI) technology provides a direct electronic interface and can convey messages and commands directly from the human brain to a computer. BCI technology involves monitoring conscious brain electrical activity via electroencephalogram (EEG) signals and detecting characteristics of EEG patterns via digital signal processing algorithms that the user generates to communicate. It has the potential to enable the physically disabled to perform many activities, thus improving their quality of life and productivity, allowing them more independence and reducing social costs. The challenge with BCI, however, is to extract the relevant patterns from the EEG signals produced by the brain each second. Recently, there has been a great progress in the development of novel paradigms for EEG signal recording, advanced methods for processing them, new applications for BCI systems and complete software and hardware packages used for BCI applications. In this book a few recent advances in these areas are discussed.

### **How to reference**

In order to correctly reference this scholarly work, feel free to copy and paste the following:

Po-Lei Lee, Yu-Te Wu, Kuo-Kai Shyu and Jen-Chuen Hsieh (2011). Brain Computer Interface Based on the Flash Onset and Offset Visual Evoked Potentials, Recent Advances in Brain-Computer Interface Systems, Prof. Reza Fazel (Ed.), ISBN: 978-953-307-175-6, InTech, Available from:  
<http://www.intechopen.com/books/recent-advances-in-brain-computer-interface-systems/brain-computer-interface-based-on-the-flash-onset-and-offset-visual-evoked-potentials>

**INTeCH**  
open science | open minds

### **InTech Europe**

University Campus STeP Ri  
Slavka Krautzeka 83/A  
51000 Rijeka, Croatia  
Phone: +385 (51) 770 447  
Fax: +385 (51) 686 166  
[www.intechopen.com](http://www.intechopen.com)

### **InTech China**

Unit 405, Office Block, Hotel Equatorial Shanghai  
No.65, Yan An Road (West), Shanghai, 200040, China  
中国上海市延安西路65号上海国际贵都大饭店办公楼405单元  
Phone: +86-21-62489820  
Fax: +86-21-62489821

© 2011 The Author(s). Licensee IntechOpen. This chapter is distributed under the terms of the [Creative Commons Attribution-NonCommercial-ShareAlike-3.0 License](https://creativecommons.org/licenses/by-nc-sa/3.0/), which permits use, distribution and reproduction for non-commercial purposes, provided the original is properly cited and derivative works building on this content are distributed under the same license.

IntechOpen

IntechOpen